Sculptured 3D twister superlattices embedded with tunable vortex spirals

Jolly Xavier,[1,*] Sunil Vyas,[1] Paramasivam Senthilkumaran,[1] Cornelia Denz,[2] and Joby Joseph[1]

[1]*Photonics Group, Department of Physics, Indian Institute of Technology Delhi, New Delhi 110016, India*

[2]*Institut für Angewandte Physik, Westfälische Wilhelms-Universität, Münster 48149, Germany*

**Corresponding author: jolly.xavierp@physics.iitd.ac.in*

Received June 16, 2011; revised July 21, 2011; accepted August 4, 2011;
posted August 5, 2011 (Doc. ID 149290); published September 1, 2011

We present diverse reconfigurable complex 3D twister vortex superlattice structures in a large area embedded with tunable vortex spirals as well as dark rings, threaded by vortex helices. We demonstrate these tunable complex chiral vortex superlattices by the superposition of relatively phase engineered plane waves. The generated complex 3D twister lattice vortex structures are computationally as well as experimentally analyzed using various tools to verify the presence of phase singularities. Our observation indicates the application-specific flexibility of our approach to tailor the transverse superlattice spatial irradiance profile of these longitudinally whirling vortex-cluster units and dark rings. © 2011 Optical Society of America

OCIS codes: 050.6875, 050.4865, 090.1970, 050.5298.

Nature expresses the "spatial order" through symmetry breakings: whether it be the translational periodicity of crystals or long range order of quasicrystals. In the recent past, the designed superposition of light fields tailored as artificial photonic lattices with periodic or transversely quasicrystallographic spatial symmetry breakings has channeled the core concepts of optics to concrete applications [1–5]. In the superposition of scalar optical wave fields, there exists the ubiquitous presence of optical vortices, the singular dislocation points or lines of amplitude nulls: the threads of absolute darkness [1,5–7]. Diverse geometries of photonic vortex lattices of varying topological charges and nondiffracting multivortex solitons have been explored [1,5–10]. But, the controlled formation of large area complex spiraling clusters of optical vortices and rings of darkness embedded in structured 3D light fields would give insight into many a future application [1,5].

Here, we report the computational as well as experimental observation of tunable vortex clusters and rings of darkness belonging to diverse reconfigurable geometries. They are embedded in complex 3D twister superlattice-structured light fields. Recently, we demonstrated 3D chiral lattices configured with both periodic as well as transversely quasicrystallographic bases by means of optical phase engineering [11]. In this Letter, we demonstrate for the first time to the best of our knowledge tunable large area 3D twister vortex superlattice (TVS) structures by means of superposition of the simplest solutions of Helmholtz equations, the plane waves. They are centrally engrafted with independently designable vortex helices surrounded by perturbed dark rings, while along these rings the zeros of real and imaginary parts of the field exactly overlap prior to unfolding. We present in a single platform the notions of transversely periodic or quasicrystallographic photonic lattices, vortex-embedded lattices as well as photonic chiral lattices [1–8,11]. We investigate the engineering of the transverse spatial irradiance profile of these complex structures as they longitudinally gyrate en masse. These real-time reconfigurable spiraling vortex superlattice structures are envisaged to find applications in advanced particle manipulation and photonic twister clusters, tunable knotted vortex structures, chiral metamaterials, dense coded satellite communications, etc. [1,5,11,12].

Usually, the combinations of complex scalar wave solutions of the form of Bessel beams, or multiple L-G modes have been used to tailor simple phase dislocation loops threaded by vortex helices [1,5,12]. Interference between an L-G beam and a Gaussian beam transforms the azimuthal phase variation into an azimuthal intensity variation [12]. In accordance with the "l" number of 2π variations in phase, "l" spiral arms could be formed. This is analogous to the unfolding of a vortex of higher order topological charge "l" into "l" singly charged vortices with identical sign in the presence of a nonsingular perturbing beam [5]. Moreover, a distribution of singly charged adjacent vortices of small localized core function of identical sign in a host Gaussian beam envelope begins to rotate as a rigid pattern [13]. Such a distribution of N vortices in a Gaussian background envelope at $z = 0$ could be expressed as a product [13,14],

$$\mathbf{E}(r, \psi, z = 0) = \mathbf{E}_0 \mathbf{E}_{\mathrm{BG}}(r) \prod_{j=1}^{N} \mathbf{A}(r_j) e^{-ikz} e^{il_j \psi_j}, \qquad (1)$$

where $\mathbf{E}_0$ is the characteristic amplitude, $\mathbf{E}_{\mathrm{BG}}$ is the background envelope function, $\mathbf{A}(r_j)$ is the small localized vortex core function of the form $\tanh(r/\omega_v)$ with ω_v defining the size of the vortex core, Ψ_j is the azimuthal coordinate in transverse plane, and k is the wave vector. Now, by an appropriate wave design of multiple interfering plane waves, diverse geometries of optical vortices similar to the above distribution can be tailored. Dynamically generated axially equidistant noncoplanar multiple plane waves with designed relative phase are superposed in a controlled manner. This forms a superlattice structure, centrally engrafted with a vortex of higher topological charge. [1,5,11]. The choice of the number and the relative initial phase of the noncoplanar plane waves to form the desired superlattice are primarily based on the required number of dark rings as well as the charge and

0146-9592/11/173512-03$15.00/0

sign of the higher order vortex at the center. In order to form a (p, q)-TVS that is threaded by p-stranded vortex helix under perturbation, we define axial dislocation strength of "p" at the center as well as "q" number of dark rings before unfolding [5]. Further, in an unperturbed structure the number of 0 to 2π phase changes along a dark ring equals the total strength of the dislocations threading it at the center. First, a combination of "n" noncoplanar plane waves is designed with $\varphi_m = [(2\pi/n) \times m]$ initial phase for the m^{th} side beam [3,11]. Then we define an integer "p" as a multiplying factor with n, leading to $g = (p \times n)$ number of noncoplanar plane waves. In order to realize 3D TVS (Fig. 1), the designed vortex superlattice structure is unfolded by an axially launched additional noncoplanar plane wave [5,11]. The overall irradiance profile of the interference pattern of $(p \times n) + 1$ linearly polarized plane waves is,

$$I(\mathbf{r}) = \sum_{i=0}^{g} |\mathbf{E}_i|^2 + \sum_{i=0}^{g} \sum_{\substack{j=0 \\ j \neq i}}^{g} \mathbf{E}_i \mathbf{E}_j^* \cdot \exp[(\mathbf{k}_i - \mathbf{k}_j) \cdot \mathbf{r} + i\varphi_{ij}], \qquad (2)$$

where $\mathbf{E}_{i,j}$ and $\mathbf{k}_{i,j}$ are the complex amplitudes, and the wave vectors respectively. φ_{ij} represents the difference in initial offset phase of the interfering beams. By taking $n = 8$ and $p = 2$, a ($p = 2$, $q = 2$)-TVS is formed, while a ($p = 3$, $q = 2$)-TVS gets formed for the values of $n = 7$ and $p = 3$. Figures 1(c), 1(d), and 2 give a detailed computational analysis of ($p = 3$, $q = 2$)-TVS by a 21+1 lattice-forming beam geometry. The complex spiral arms are formed while the generated TVS lattice-forming wave is superposed with a spherical wave [Fig. 1(d)]. The optical vortices occur at the intersection lines of the surfaces given by the Re$E(r)$ and the Im$E(r)$ zeros [Figs. 2(c) and 2(d)] [15]. In the unperturbed lattice structure before unfolding, only along the two dark rings ($q = 2$) that surround the central higher order vortex, the zeros of Re$E(r)$ and Im$E(r)$ exactly overlap on each other [Fig. 2(c)]. The computed phase patterns show 2π phase variations leading to phase dislocations, indicating the singular nature of the intensity nodes as given in the insets of Figs. 2(c) and 2(d).

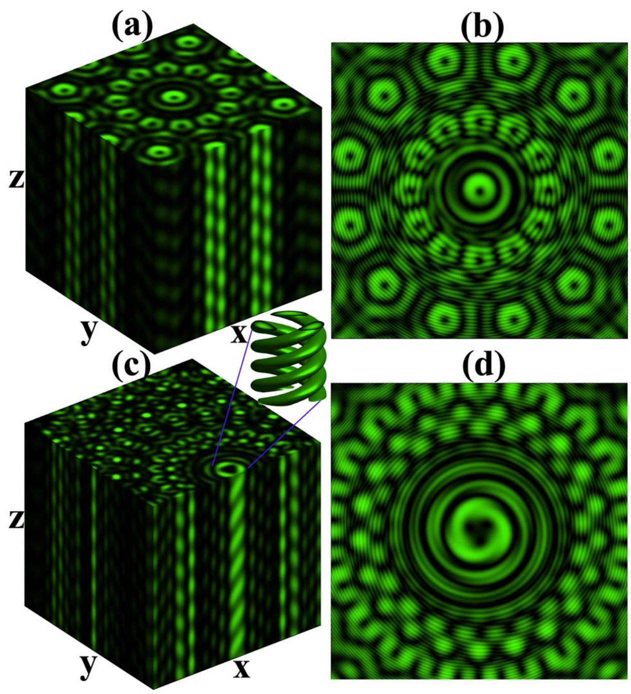

Fig. 1. (Color online) (a) 3D intensity distribution of transversely 12-fold symmetry spiraling TVS by $12 + 1$ interfering beams. Media 1 (b) x-y plane of the structure while TVS lattice-forming wave is superposed with a spherical wave. (c) and (d) Respectively for ($p = 3, q = 2$) TVS by $21 + 1$ interfering beams. Media 2

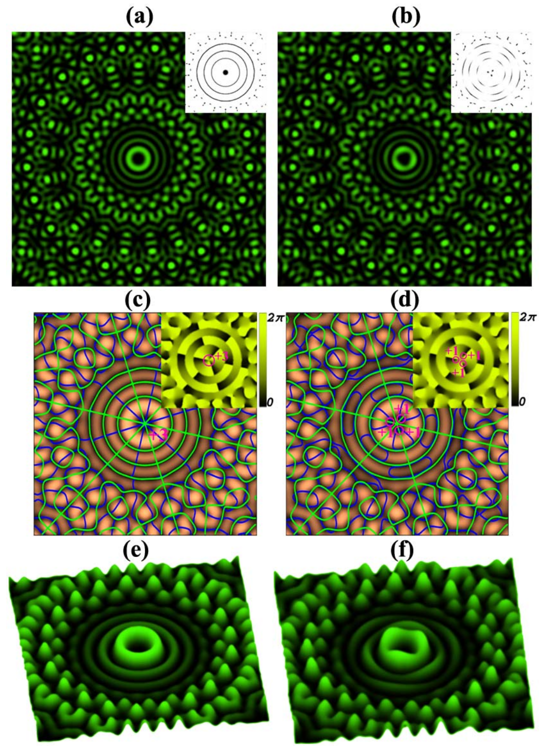

Fig. 2. (Color online) Computer analysis of ($p = 3, q = 2$) TVS. Left column: folded structure. Right column: unfolded structure. (a)–(b) Intensity distribution in x-y plane (Inset: Distribution with a lower threshold value). (c)–(d) Zero crossing: Zeros of Re$E(r)$ [blue] and Im$E(r)$ [green] (Inset: Phase profile). (e)–(f) Intensity mesh plots.

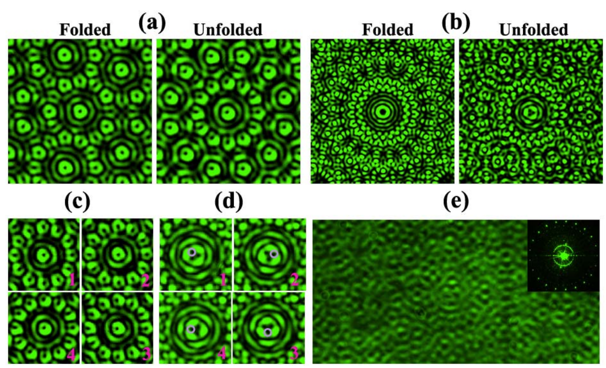

Fig. 3. (Color online) Experimental realization of TVS. (a) x-y plane of the intensity profile of transversely 12-fold symmetry spiraling TVS. (b) For ($p = 3$, $q = 2$) TVS. (c)–(d) Spiraling structures of (a) and (b) as z value is varied. (e) Recorded image of the x-y plane of the real lattice of (b) fabricated in SBN: Ce PR material (Inset: Far field diffraction pattern).

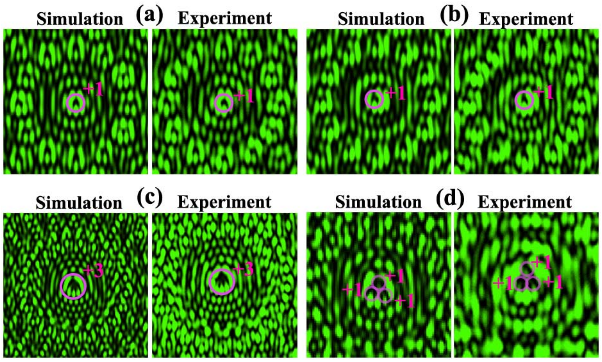

Fig. 4. (Color online) The fork formation while the TVS lattice-forming wave is interfered with a plane wave launched at a large angle from the axis. (a) and (c): folded, (b) and (d): unfolded. (a)–(b): Transversely 12-fold symmetry TVS. (c)–(d): ($p = 3$, $q = 2$) TVS.

In Figs. 3 and 4, we demonstrate well-matched experimental results to those of our computations. We realize this by means of a phase only spatial light modulator (SLM) (Holoeye PLUTO-VIS, Holoeye Photonics AG) assisted single step fabrication approach as given in [3,4,11]. Imaging the multiple transverse x-y planes for varying values of z along the direction of propagation revealed the spiraling nature of the complex 3D TVS [Fig. 3(c) and 3(d)]. Further, we also made use of a $5\,\mathrm{mm} \times 5\,\mathrm{mm} \times 5\,\mathrm{mm}$ Cerium doped $Sr_{0.60}Ba_{0.40}Nb_2O_6$ (SBN:Ce) photorefractive (PR) crystal as one of the recording photosensitive materials for the demonstration of the generated lattices as given in Fig. 3(e). PR is externally biased by an applied static electric field of 1.6–2 kV/cm in a self-defocusing mode [8,9]. The generated structures in PR medium could also be fine tuned by modifying in-plane spatial position of the interfering beams in consideration of the orientational anisotropy of the PR medium [4,10]. In addition to capturing the intensity distributions, the experimental realization of the forks (Fig. 4), well matching to the simulated results clearly indicate the position as well as the topological charge and sign of the cyclic phase change around the intensity nodes of designed vortices. The fork formation at the center in the folded and the unfolded TVS structure gives the inference of the identical sign of the single charged vortices in the presence of a perturbing field [1,5,10]. Further we extend our investigation to very complex TVS lattices. For brevity, as given in Fig. 5, we show here ($p = 6$, $q = 4$) TVS by $36 + 1$ lattice-forming beams, where $n = 6$.

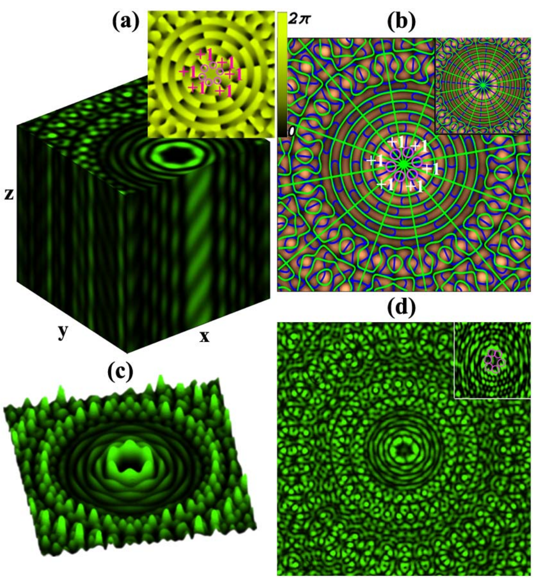

Fig. 5. (Color online) Computational and experimental analysis of ($p = 6$, $q = 4$) TVS. (a) 3D intensity distribution (Inset: Phase profile). (b) Zero crossing plot: Zeros of Re$E(r)$ [Blue] and Im$E(r)$ [Green] (Inset: For the folded structure). (c) Intensity mesh plot. (d) Experimentally realized intensity distribution of ($p = 6$, $q = 4$) TVS x-y plane (Inset: The fork formation).

We have demonstrated diverse large area spiraling 3D TVS, centrally configured with tailored dark rings of diverse order threaded by vortex helices, by the designed interference of relatively phase engineered plane waves. Through a programmable SLM-assisted single step fabrication approach, well-defined diverse structures of 3D TVS are experimentally realized and analyzed. We envisage also the formation of large area superlattices embedded even with vortex knots of diverse tunable orders [5,16], which is under our current investigation, by further tuning the sculptured helices and rings of darkness evolving in these 3D gyrating superlattices by means of relatively phase engineered multiple plane wave interference.

The present project is supported by the Indian Institute of Technology, Delhi, India.

References

1. D. L. Andrews, *Structured Light and Its Applications: An Introduction to Phase-Structured Beams and Nanoscale Optical Forces* (Academic, 2008).
2. T. Kondo, S. Juodkazis, V. Mizeikis, and H. Misawa, Opt. Express **14**, 7943 (2006).
3. J. Xavier, P. Rose, B. Terhalle, J. Joseph, and C. Denz, Opt. Lett. **34**, 2625 (2009).
4. J. Xavier, M. Boguslawski, P. Rose, J. Joseph, and C. Denz, Adv. Mater. **22**, 356 (2010).
5. M. R. Dennis, K. O'Holleran, and M. J. Padgett, Prog. Opt. **53**, 293 (2009).
6. Y. F. Chen, H. C. Liang, Y. C. Lin, Y. S. Tzeng, K. W. Su, and K. F. Huang, Phys. Rev. A **83**, 053813 (2011).
7. L. G. Wang, L. Q. Wang, and S. Y. Zhu, Opt. Commun. **282**, 1088 (2009).
8. S. Jia and J. W. Fleischer, Phys. Rev. A **79**, 041804 (2009).
9. D. Buccoliero, A. S. Desyatnikov, W. Krolikowski, and Y. S. Kivshar, Opt. Lett. **33**, 198 (2008).
10. B. Terhalle, D. Göries, T. Richter, P. Rose, A. S. Desyatnikov, F. Kaiser, and C. Denz, Opt. Lett. **35**, 604 (2010).
11. J. Xavier, and J. Joseph, Opt. Lett. **36**, 403 (2011).
12. L. Paterson, M. P. MacDonald, J. Arlt, W. Sibbett, P. E. Bryant, and K. Dholakia, Science **292**, 912 (2001).
13. G. Indbetouw, J. Mod. Opt. **40**, 73 (1993).
14. P. Senthilkumaran, F. Wyrowski, and H. Schimmel, Opt. Lasers Eng. **43**, 43 (2005).
15. I. Freund and N. Shvartsman, Phys. Rev. A **50**, 5164 (1994).
16. J. Leach, M. R. Dennis, J. Courtial, and M. J. Padgett, New J. Phys. **7**, 55 (2005).